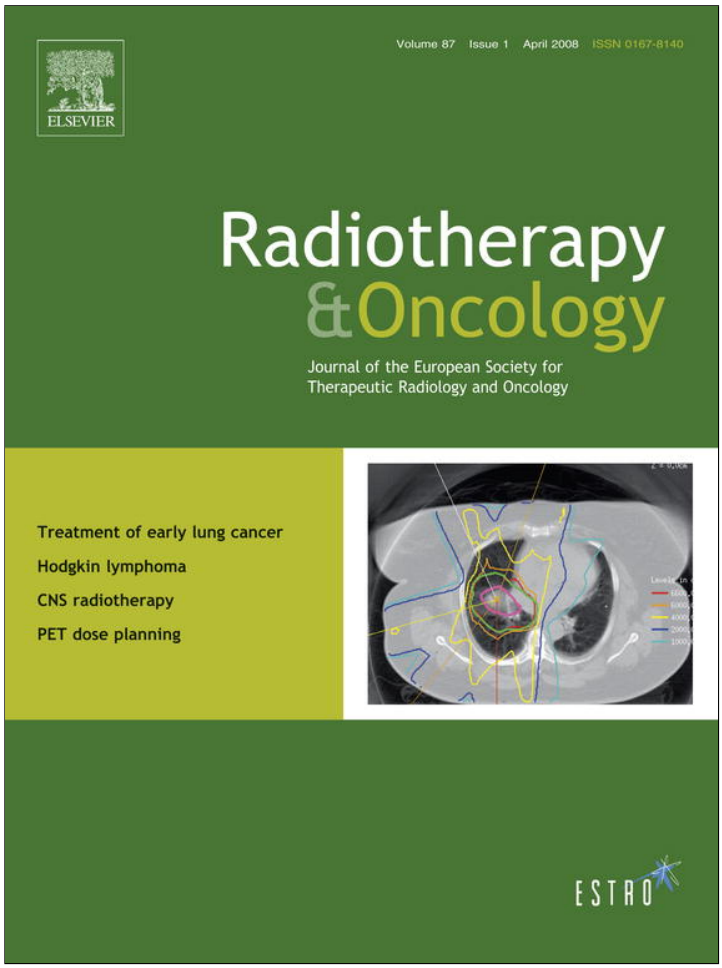

Radiotherapy and Oncology 87 (2008) 147—151
www.thegreenjournal.com

Micro-PET in rodents

Immobilization device for *in vivo* and *in vitro* multimodality image registration of rodent tumors

Nicolas Christian[a], John A. Lee[a], Anne Bol[a], Marc De Bast[a], Bernard Gallez[b], Vincent Grégoire[a,*]

[a]*Center for Molecular Imaging and Experimental Radiotherapy, and* [b]*Biomedical Magnetic Resonance Unit, Université Catholique de Louvain, Brussels, Belgium*

Abstract

Biological image-guided radiotherapy requires that PET accurately identifies biologically relevant sub-volumes within a tumor. In this framework, an immobilization device was developed to study multi-imaging (CT, micro-MRI, micro-PET, and autoradiography) registration of mouse tumors. The registration accuracy assessed by calculating the average minimal distance between two skew lines was in the order of 0.2—0.3 mm.
 Radiotherapy and Oncology 87 (2008) 147—151.

Keywords: Mouse tumor; Image registration; Micro-PET; MRI; CT; Autoradiography

Adaptive image-guided radiotherapy aims at re-assessing dose distributions as a function of target volume modifications during the course of treatment. In this framework, functional imaging with positron emission tomography (PET) using various tracers may be relevant to identify biological sub-volumes, which might require additional dose delivery. As a prerequisite for this approach, PET image acquisition should be sensitive and specific enough to trace spatial changes and modifications in the signal intensity throughout the treatment. Despite improvements in PET cameras, data processing and image reconstruction algorithms, the resolution and sensitivity of PET systems are still the limiting factors, and uncertainties remain regarding correlations between the *in vivo* images and the biological phenomena at the molecular level. In this framework, the use of animal models is of growing interest. Few studies have already been reported on image fusion between CT, MRI and PET images in small animals [1—3]. However, the validation of functional imaging for adaptive radiotherapy requires one step further, which is a direct comparison between *in vivo* and *in vitro* imaging modalities.

Mutual information based algorithms have already been developed for image registration of *in vivo* data and histological sections [4—6]. However, for high accuracy registration, these methods require similarities between the two data sets, e.g. anatomical information, which can doubtfully be obtained from PET images. Consequently, a fiduciary-based approach is required for multimodality image registration including PET data.

Devices using fiduciary markers have already been described for image registration between *in vivo* and *in vitro* modalities. In the first device ever developed [7], hollow rods were inserted into the tumor. Those rods were visualized in all modalities, allowing image registration. However, the insertion of material into the tumor could possibly affect the tumor physiology and is thus a limiting factor of this technique. Another device [8] was based on a wooden framework to which both the mouse and the markers were attached. The first step of the process was a freezing step with cold nitrogen gas. CT and PET imaging were then performed. The mouse was then packed in carboxymethylcellulose and frozen overnight, then sliced. Due to the initial freezing step, MR imaging could not be performed with this device. Moreover, due to the long freezing time, autoradiography with ^{18}F-tracers was no more feasible on the tissue sections.

The aim of the present study was to develop a multipurpose immobilization device for *in vivo* (CT, MRI, and PET) and *in vitro* (autoradiography) multimodality image registration of mouse tumors. This device had to fulfill several constraints: it should offer high registration accuracy (submillimeter) and reproducibility between *in vivo* and *in vitro* modalities, without altering the tumor metabolism; moreover, the animals have to stay alive throughout the whole procedure to allow the possibility of inducing metabolic changes (e.g. modulation of tumor oxygenation or proliferation) during the experiment. Last, the whole procedure should be fast enough to perform autoradiography imaging of the tracer used for *in vivo* PET imaging.

0167-8140/$ - see front matter doi:10.1016/j.radonc.2008.02.016

Materials and methods

Animal and tumor model

Eight to 10-week-old male C3H/HeOuJIco (IFFA Credo Belgium) mice were used in this study. Animals were maintained in a facility approved by the Belgian Ministry of Agriculture in accordance with current regulations and standards. Animals were housed 4—5 per cage and fed *ad libitum*. FSA II fibrosarcoma syngeneic to C3Hf/Kam mice were generated in the right thigh. These tumors were kindly provided by Dr. L. Milas from the University of Texas, M.D. Anderson Cancer Center, Houston, USA. Maintenance and expansion were done as previously described [9]. Tumor growth was determined by daily measurements of the three orthogonal diameters with a caliper. Experiments were performed on 10—12 mm mean diameter tumors. The tumor-bearing leg and the back skin were depilated with a hair removal cream (Veet, Reckitt Benckiser).

When requested, animals were anesthetized with an i.p. injection of 80 mg/kg of ketamine (Ketalar®, Parke-Davis, Warner Lambert S.A., Belgium) and 8 mg/kg of xylazine (Rompun®, Bayer AG, Germany). This induction was followed by hourly subcutaneous (in the neck) injections of 20 mg/kg of ketamine. Animals were not anaesthetized for more than 2 h.

All the experiments were supervised and approved by the ethic committee on animal experimentation of the medical school of the Université Catholique de Louvain. The ''Principles of laboratory animal care'' (NIH publication No. 86-23, revised 1985) were strictly followed.

Immobilization and *in vivo* imaging

A Styrofoam® (Styrofoam Roofmate SL-X, Dow Chemical, USA) immobilization device was designed for each animal (Fig. 1a). It consisted of an excavated cylinder of 5.5 cm in height and 7 cm in diameter. The external diameter corresponded to the largest diameter of the Bruker Biospec whole body antenna. One end of the cylinder was closed with adhesive tape. A Styrofoam® thin plate of $2 \times 60 \times 120$ mm with longitudinal incisions was inserted into the device.

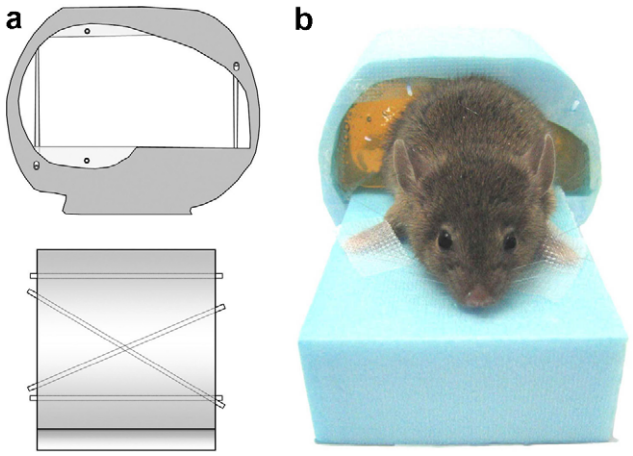

Fig. 1. Immobilization device. (a) Schematic drawing of the Styrofoam® cylinder mould illustrating the 4 rods position in sagittal and transversal views. (b) View of the immobilization device with a mouse embedded from the belt onward in the gelatin. The mouse could breath normally throughout the experiments.

Four 6 cm long Teflon® tubes with internal sections of 0.4 mm containing metallic wires were placed inside the mould to generate a reference coordinate system. Two tubes were placed on top of each other in the sagittal plane parallel to the cylinder axis; the two other tubes were set skewed, in the transversal plane, on the left and the right side of the device.

An anesthetized mouse was gently taped on the Styrofoam® plate with its legs spread apart. The plate was positioned inside the device. A hole was drilled in the adhesive tape at the closed end of the cylinder for the mouse's tail. A water solution of 10% glycerol (CERTA, Braine-l'Alleud, Belgium) and 20% gelatin (Gelatin powder Ph. Eur., VWR) was prepared and maintained in a water bath at 32 °C. A mean activity of 18.5 kBq/ml (0.5 μCi/ml) of [^{18}F]-FDG was added to the mixture, which was then gently poured in the mould allowing for the immersion of the fiducial markers and the animal from its pelvis downward. During the whole procedure, the animal was allowed normal free breathing. After a few minutes at room temperature, the gelatin had solidified and the device could be easily handled (Fig. 1b). The wires were then removed from the Teflon® tubes, and the tubes were filled with oil or with a mix of iodine contrast agent (Telebrix 35, Guerbet, France) and radioactive ^{18}F-tracer at a concentration of 9.25 MBq/ml (250 μCi/ml), allowing their visualization on MRI, CT and PET, respectively. The entire set-up procedure was performed in less than 1 h.

Mice were kept anesthetized on the immobilization device for the whole duration of the image acquisition. CT images were acquired on a 16-detector row spiral computed tomography (Mx8000 IDT, Philips Medical Systems) using a field of view of 75 mm, a 0.5 mm slice thickness, a reconstruction interval of 0.5 mm and a pitch of 0.125. The full width at half-maximum (FWHM) of the PSF was 0.48 mm. Axial images were acquired using a matrix of $512 \times 512 \times 80$ with a voxel size of $0.1465 \times 0.1465 \times 0.5$ mm^3 in the *x*, *y* and *z* direction, respectively. MRI images were acquired on a 4.7 T (200 MHz, 1H), 40 cm inner diameter bore system (Bruker Biospec, Ettlingen, Germany). T2-weighted images were acquired using a fast spin echo sequence (repetition time = 4.7, echo time = 12 ms, N averages = 8, RARE factor = 8). The total acquisition time was, on average, 10 min. A birdcage radiofrequency coil with an inner diameter of 60 mm was used for radiofrequency transmission and reception. Axial images were acquired using a matrix of $128 \times 128 \times 40$, with a voxel size of $0.469 \times 0.469 \times 1.0$ mm^3 in the *x*, *y* and *z* direction, respectively. For the PET images, the mouse was injected with 11.1 MBq (300 μCi, 11.1 MBq) of [^{18}F]-FDG through the tail vein and, after 30 min rest, a 10 min static acquisition was performed on a dedicated small-animal PET scanner (Mosaic, Philips Medical Systems, Cleveland) with a FWHM of 2.5 mm. Transmission scans were then acquired in single mode using a 370 MBq ^{137}Cs source for attenuation correction. All images were reconstructed with a full-3D iterative algorithm (3D-RAMLA) [10]. Axial images were acquired using a matrix of $128 \times 128 \times 120$, with a voxel size of 1 mm^3.

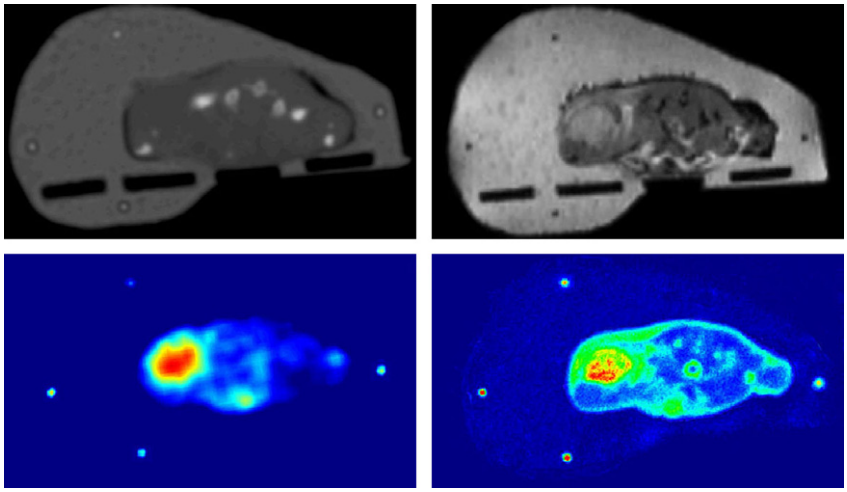

Fig. 2. Transversal view of the immobilization device imaged with CT, MRI, PET and autoradiography. The Teflon® tube sections are clearly visible on all modalities.

In vitro imaging, image processing and data analysis

After PET imaging, the anesthetized mouse was euthanized with a lethal dose of pentobarbital (200 mg/kg) injected s.c. in the neck. The mouse containing device was then frozen at −25 °C for 5 h. The entire device could then be sliced (Universal slicer MA9101, Bosch, Germany), perpendicular to the cylinder axis. During the slicing procedure, slices were kept in an −80 °C refrigerated box. The length of the block was measured when slicing reached the beginning and the end of the volume of interest. The length was divided by the number of slices to obtain the mean slice thickness, which on average reached 0.92 ± 0.07 mm (mean ± 2 SD) for the 5 mice that underwent the full procedure. The material loss during the slicing was estimated between 0.08 and 0.1 mm per slice. This thickness is the lower limit that could be obtained with the device without damaging the slices.

Each slice was then exposed at −25 °C for 30 min to a phosphor storage plate (BAS-MS 2025, Fuji Photo Film Co., Japan). The ^{18}F distribution image was then digitalized using a fluorescent image analyzer (FLA-5100, Fuji Photo Film Co., Japan) with a scan resolution of 100 μm. The images were saved in true color TIFF format for further analysis.

The slices were then transferred to a cryostat chamber, and on each slice, the tumor area was gently excised with a scalpel and removed from the surrounding tissues and gelatin. The 0.9 mm thick tumor pieces were cut with a cryostat to obtain 10 μm thick slices. These sections were also exposed to a phosphor storage plate and digitized using the fluorescent image analyzer with a similar resolution of 100 μm. The corresponding slices were easily registered on visual basis for further comparison.

The TIFF file containing the ^{18}F distribution of all slices was imported in a home made software. This software allowed the user to select and sort the slices with a few mouse clicks. After the selection, the slices were automatically stacked in the proper order and a marker-based registration aligned them automatically according to the positions of the Teflon® tubes. The resulting volume was exported in an ECAT 7 file. Voxel size was 100 μm in both *x* and *y* directions and 0.92 mm in *z* direction. The accuracy of the reconstruction of the autoradiography volume was evaluated by the root mean square error (RMSE) of the linear fit of the Teflon® tube alignment. For the quantification of the radioactivity within the tumors, a normalization factor was used to take into account the small difference in slide thickness as explained in Results.

CT, MR, PET and autoradiography images were imported in ECAT format into the PMod 2.6 fusion module (Pmod Technologies Ltd., Switzerland) for manual registration using the Teflon® tubes as reference system. On all imaging modalities, the Teflon® tubes were clearly visible on axial, coronal and sagittal planes (Fig. 2). Before registration, CT, MR and PET images were rescaled to the CT voxel size, i.e. $0.1465 \times 0.1465 \times 0.5\ \text{mm}^3$. For the registration between PET images and autoradiography, images were rescaled to the autoradiography voxel size, i.e. $0.1 \times 0.1 \times 0.92\ \text{mm}^3$.

The registration accuracy was performed by calculating the distance and the angle between the Teflon® tubes on each pair of imaging modalities. On each modality, the Teflon® tubes were reconstructed from the axial images by manually selecting the central voxel of each tube. The rods were then modeled by a linear equation using a least square fit. Corresponding rods were compared on pairs of imaging modalities (e.g. CT-MR, CT-PET,...); minimal distances between corresponding rods (assessing translation misalignments) and angle between the direction vectors of the rods (assessing rotation misalignments) were then computed. These values were averaged for the four pairs of rods within a set of two imaging modalities to assess the global quality of registration.

Results and discussion

The alignment of the various autoradiography slices was quite accurate with an average root mean square error of 0.2 mm. The registration accuracy between the various

imaging modalities including the autoradiography was also very good. On average, translation misalignment reached 0.2 mm for all four pairs of comparisons (Table 1). The rotation error was also very low, reaching a maximum of 3.5° for PET—autoradiography registration.

Our data compare well with other repositioning devices for small animals. In the method developed by Humm et al. [7], the registration accuracy of 0.20 mm was achieved between MRI and PET image. The digitized autoradiography sections were registered with three-dimensional MRI images with an average accuracy of 0.33 mm. In another device [11], expending foam was used to build animal-specifics molds for immobilization and reproducible positioning. The mould was then used to replace the animal for multiple PET acquisitions with different tracers. Both images were easily registered and compared. However, in this model, no assessment of repositioning accuracy was performed; it was estimated by the authors in the order of 1—2 mm. Moreover, this device did not allow the realization of autoradiography.

Our device has several advantages compared to other devices. First, it is non-traumatic for the tumor microenvironment as no marker or rod has to be implanted in the tumor. Second, since the animals can be maintained alive for several hours without major perturbations of their physiology, this device is particularly suitable for re-imaging animals, in which metabolic changes (e.g. proliferation, oxygenation) have been artificially induced. In this initial set-up, temperature of the animal was not monitored. However, this could easily be done using a thermo-probe positioned on the back of the mouse. Third, the whole process is fast enough to allow autoradiography of the mouse sections.

In the design and the development of this small-animal repositioning device, a special attention was drawn on several parameters.

First, the embedding material used needed to fulfill several requirements. It needed to be poured around the animal without any harm (e.g. no risk of skin burn) and it had to solidify at room temperature. It also needed to homogeneously freeze and be easily sliced. A gelatin solution at 32 °C fulfilled all these conditions, except that it inflated due to crystallization during the freezing procedure, thus hampering proper registration between the autoradiography and PET images. After several tests, it was found that adding 10% of glycerol, which can limit water crystallization, could correct for this drawback. Volume expansion of freezing water is around 10%. By adding 10% glycerol, the volume expansion was approximately reduced to 4.5%. Adding more glycerol resulted in less volume expansion but decreased the toughness of gelatin, impairing the slicing process. An adequate freezing procedure also needed to be tuned to the use of gelatin. When using liquid nitrogen, the whole device was frozen in approximately 15 min. The drawback was the extreme hardness of gelatin at such extremely low temperature, prohibiting the slicing step. When waiting for warming up, cracks appeared in the gelatin. The same problem was observed with dry ice. Finally, the only adequate temperature for efficient slicing was around −25 °C, therefore conditioning the whole freezing procedure.

Due to the difficulty to be exactly constant in the slicing, a second difficulty resided in a slight variation of the thickness of the slices used for autoradiography. Consequently, heterogeneities in the quantification of radioactivity throughout the volumes of interest were observed. This effect was quantified by slicing and imaging a homogeneously radioactive gelatin block (3.7 MBq/ml). When measuring the radioactivity in regions of interest drawn in 10 contiguous slices, a 17% coefficient of variation between slices was found (mean/SD). This variation resulted from a slightly higher activity in ticker slices and a slightly lower activity in thinner slices. Such variability was also observed for tumor-bearing mice sections. Due to the difficulty in accurate slice thickness measurement, a simple calibration curve was not applicable. Five phantoms made up of a high radioactivity (14.8 MBq) spheres (10 mm in diameter) surrounded by a low radioactivity (3.9 MBq) background were studied to solve this problem. The phantoms were frozen and sliced using the same procedure as for the animals to obtain 10 contiguous slices per phantom. An autoradiography of each slice was performed and quantified. For the five phantoms, the coefficient of variation of the radioactivity in the high activity spheres was 6.1 ± 1.9% (mean ± 2 SD). However, on average, on a slice-by-slice basis, there was a very good correlation ($r = 0.94$) between the low activity (i.e. the background) and the high activity (i.e. the spheres), indicating that this thickness effect was present throughout the slices irrespective of the level of radioactivity. The background activity could therefore be used as an internal standard to calibrate the activity within the sphere. The activity in the background was measured and a multiplicative factor was then applied on each slice to normalize the background activity between the slices. After this normalization, the background activity was even in all the slices and the activity within the spheres was also modified by this multiplicative factor. When such procedure was applied, the coefficient of variation of the radioactivity of the spheres decreased to 3.5 ± 1% (mean ± 2 SD), confirming that the normalization of the heterogeneities between the low activity regions successfully reduced the measured variations in the high activity spheres. For the animal data, a similar correction procedure was applied. [^{18}F]-FDG was added to the gelatin surrounding the animals (18.5 kBq/ml). Then, before quantifying the radioactivity in the tumors on autoradiography images, the activity in the background was calculated and normalized, thus modifying the activity within the tumor.

Table 1
Registration accuracy between CT, MR, PET and autoradiography images

	MR-CT (mean ± SD)	PET-CT (mean ± SD)	PET-MR (mean ± SD)	PET—autoradiography (mean ± SD)
Translation misalignment (mm)	0.21 ± 0.06	0.23 ± 0.12	0.28 ± 0.07	0.18 ± 0.04
Rotation misalignment (°)	2.2 ± 0.3	2.5 ± 0.7	2.5 ± 0.5	3.5 ± 0.4

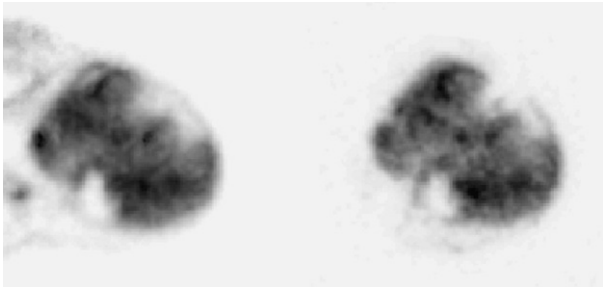

Fig. 3. Autoradiography images of a 0.9 mm thick slice (left) and its corresponding 10 μm section (right). Pixel size in both images was 100 μm. The correlation coefficient of the pixel-by-pixel analysis for these two slices was 0.94.

A last issue resided in the slice thickness on the autoradiography, which could cause image blurring and resolution degradation due to the spreading of the gamma rays on the phosphor storing plate. The slicing technique was responsible for the limitation in slice thickness that could not be decreased below 0.9 mm. To study this phenomenon, the autoradiography of 900 μm (slice thickness of the frozen animals) slices was compared to the autoradiography of 10 μm slices cut from the same section, both using a pixel size of 100 μm. From the 5 mice that underwent the whole imaging procedure, a total of 10 ''thin–thick'' comparisons were obtained. The pairs of images were then registered on a visual basis. Due to the high similarity between the 900 and 10 μm sections, the registration could be easily achieved (Fig. 3) and pixel-by-pixel analysis of radioactivity was performed. On average, the correlation between radioactivity from the thick and thin images reached 0.85 ± 0.05, confirming the good visual registration between the two sets of images.

In conclusion, the immobilization device described in this study allows for high-resolution registrations between *in vivo* and *in vitro* images. This non-traumatic device permits animal's immobilization at the level of the tumor implantation, while allowing mice to breath normally. The first application of this device will be the validation of [^{18}F]-FDG distribution on several mice tumor models under different physiological conditions.

Acknowledgements

Nicolas Christian is a research fellow of the ''Fonds pour la formation à la Recherche dans l'Industrie et l'Agriculture (F.R.I.A.)'' of Belgium. The project was supported by a grant from the ''Fonds Joseph Maisin'', Brussels, Belgium, by the European Commission's Sixth Framework Programme funding (Contract No. LSHC-CT-2004-505785), and by a program project from the ''Institut National du Cancer'' of France (Project INCa N° RS 020).

* **Corresponding author. Vincent Grégoire**, Department of Radiation Oncology, Cliniques Universitaires Saint-Luc, Avenue Hippocrate, 10, B-1200, Brussels, Belgium. *E-mail address:* vincent.gregoire@uclouvain.be

Received 31 August 2007; received in revised form 14 February 2008; accepted 14 February 2008; Available online 24 March 2008

References

[1] Chow PL, Stout DB, Komisopoulou E, Chatziioannou AF. A method of image registration for small animal, multi-modality imaging. Phys Med Biol 2006;51:379–90.

[2] Rowland DJ, Garbow JR, Laforest R, Snyder AZ. Registration of [^{18}F]FDG microPET and small-animal MRI. Nucl Med Biol 2005;32:567–72.

[3] Jan ML, Chuang KS, Chen GW, Ni YC, Chen S, Chang CH, et al. A three-dimensional registration method for automated fusion of micro PET-CT-SPECT whole-body images. IEEE Trans Med Imaging 2005;24:886–93.

[4] Breen MS, Lazebnik RS, Wilson DL. Three-dimensional registration of magnetic resonance image data to histological sections with model-based evaluation. Ann Biomed Eng 2005;33:1100–12.

[5] du Bois d'Aische A, Craene MD, Geets X, Gregoire V, Macq B, et al. Efficient multi-modal dense field non-rigid registration: alignment of histological and section images. Med Image Anal 2005;9:538–46.

[6] Meyer CR, Moffat BA, Kuszpit KK, Bland PL, Mckeever PE, Johnson TD, et al. A methodology for registration of a histological slide and in vivo MRI volume based on optimizing mutual information. Mol Imaging 2006;5:16–23.

[7] Humm JL, Ballon D, Hu YC, Ruan S, Chui C, Tulipano PK, et al. A stereotactic method for the three-dimensional registration of multi-modality biologic images in animals: NMR, PET, histology, and autoradiography. Med Phys 2003;30:2303–14.

[8] Dogdas B, Stout D, Chatziioannou A, Leahy RM. Digimouse: a 3D whole body mouse atlas from CT and cryosection data. Phys Med Biol 2007;52:577–87.

[9] Milas L, Hunter N, Mason K, Withers HR. Immunological resistance to pulmonary metastases in C3Hf-Bu mice bearing syngeneic fibrosarcoma of different sizes. Cancer Res 1974;34:61–71.

[10] Daube-Witherspoon ME, Matej S, Karp JS, Lewitt RM. Application of the row action maximum likelihood algorithm with spherical basis functions to clinical PET imaging. IEEE Trans Nucl Sci 2001;48:24–30.

[11] Zanzonico P, Campa J, Polycarpe-Holman D, et al. Animal-specific positioning molds for registration of repeat imaging studies: comparative microPET imaging of F^{18}-labeled fluorodeoxyglucose and fluoro-misonidazole in rodent tumors. Nucl Med Biol 2006;33:65–70.